



HAL
open science

Profiling the intragenic toxicity determinants of toxin–antitoxin systems: revisiting hok / Sok regulation

Anaïs Le Rhun, Nicolas Tourasse, Simon Bonabal, Isabelle Iost, Fanny Boissier, Fabien Darfeuille

► To cite this version:

Anaïs Le Rhun, Nicolas Tourasse, Simon Bonabal, Isabelle Iost, Fanny Boissier, et al.. Profiling the intragenic toxicity determinants of toxin–antitoxin systems: revisiting hok / Sok regulation. *Nucleic Acids Research*, 2022, 10.1093/nar/gkac940 . hal-03872182

HAL Id: hal-03872182

<https://hal.science/hal-03872182v1>

Submitted on 30 Nov 2022

HAL is a multi-disciplinary open access archive for the deposit and dissemination of scientific research documents, whether they are published or not. The documents may come from teaching and research institutions in France or abroad, or from public or private research centers.

L'archive ouverte pluridisciplinaire **HAL**, est destinée au dépôt et à la diffusion de documents scientifiques de niveau recherche, publiés ou non, émanant des établissements d'enseignement et de recherche français ou étrangers, des laboratoires publics ou privés.

Profiling the intragenic toxicity determinants of toxin–antitoxin systems: revisiting *hok/Sok* regulation

Anaïs Le Rhun¹*, Nicolas J. Tourasse, Simon Bonabal, Isabelle Iost, Fanny Boissier and Fabien Darfeuille¹*

Univ. Bordeaux, CNRS, INSERM, ARNA, UMR 5320, U1212, F-33000 Bordeaux, France

Received July 18, 2022; Revised September 15, 2022; Editorial Decision October 06, 2022; Accepted October 20, 2022

ABSTRACT

Type I toxin–antitoxin systems (T1TAs) are extremely potent bacterial killing systems difficult to characterize using classical approaches. To assess the killing capability of type I toxins and to identify mutations suppressing the toxin expression or activity, we previously developed the FASTBAC-Seq (Functional Analysis of Toxin–Antitoxin Systems in Bacteria by Deep Sequencing) method in *Helicobacter pylori*. This method combines a life and death selection with deep sequencing. Here, we adapted and improved our method to investigate T1TAs in the model organism *Escherichia coli*. As a proof of concept, we revisited the regulation of the plasmidic *hok/Sok* T1TA system. We revealed the death-inducing phenotype of the Hok toxin when it is expressed from the chromosome in the absence of the antitoxin and recovered previously described intragenic toxicity determinants of this system. We identified nucleotides that are essential for the transcription, translation or activity of Hok. We also discovered single-nucleotide substitutions leading to structural changes affecting either the translation or the stability of the *hok* mRNA. Overall, we provide the community with an easy-to-use approach to widely characterize TA systems from diverse types and bacteria.

INTRODUCTION

Many bacteria encode lethal proteins in their genome alongside antidotes that are able to counteract their toxicity. These toxin–antitoxin (TA) systems are classified into different types according to the nature of the antitoxins and the mechanism of action of the toxin, extensively reviewed by Harms *et al.* (1). Type I TA systems (T1TAs) are RNA/RNA interacting systems. The antitoxin RNA, encoded on the opposite strand of the toxin mRNA, acts as a noncoding antisense RNA, mediating translation inhibi-

tion and/or mRNA degradation (2). The genomic location of predicted and validated T1TAs can be found in the T1TA database (db) that we recently developed (3).

The *hok/Sok* system has been the most studied T1TA. It was first discovered on *Escherichia coli* R1 plasmid where it acts by maintaining plasmid copies in a cell population through post-segregational killing of the plasmid-free cells (4,5). The Hok (host-killing) type I toxin is a small hydrophobic protein [52 amino acids (aa)] targeting the inner membrane and leading to cell death. The Sok (suppression of killing) antitoxin is an RNA that inhibits the production of Hok at the post-transcriptional level (6,7). The system is composed of a third gene, *mok* (modulation of killing), that overlaps with the *hok* coding sequence (CDS) and is required for *hok* translation (6). Indeed, the translation of *mok*, rather than the Mok product, was shown to be important for proper *hok* regulation and expression (6). For simplicity, the *mok-hok* bicistronic mRNA will be referred to as the *hok* mRNA throughout this paper.

Pioneering studies have demonstrated that *hok* mRNA translation requires a conformational switch between a full-length (FL) *hok* mRNA (translationally inactive) and a truncated (Tr) *hok* mRNA structure (translationally active) (8,9). First, a long-distance interaction between the 5' and the 3' untranslated regions (UTRs) strongly stabilizes the closed FL-*hok* mRNA. This interaction, described as the 'translational activator element'/'fold-back inhibitory element' (tac/fbi) stem, prevents translation by sequestration of the Shine–Dalgarno sequence (SD) of *mok* by an 'upstream complementary box' (ucb) (9). Then, the *hok* mRNA undergoes a slow maturation at the 3' end, triggering a structural rearrangement that renders the Tr-*hok* mRNA translatable by the formation of a tac/ucb stem and a *mok* SD/'downstream complementary box' (dcb) stem (10). Not only this rearrangement frees the *mok* SD for translation, it also allows the binding of the Sok RNA antitoxin (6,10). This binding entails rapid degradation of the *hok* mRNA/Sok RNA duplex by RNase III (10,11). In addition, to avoid co-transcriptional translation, a transient metastable structure is formed before the *hok* mRNA is fully

*To whom correspondence should be addressed. Tel: +33 557574565; Email: anaïs.le-rhun@inserm.fr
Correspondence may also be addressed to Fabien Darfeuille. Tel: +33 557571014; Email: fabien.darfeuille@inserm.fr

transcribed, where the *tac* element pairs with a complementary region immediately downstream (12).

TITAs have been predicted in pathogenic bacteria both *in silico* and from transcriptomic studies (e.g. *Helicobacter pylori*, *Clostridioides difficile*, *Staphylococcus aureus*) (13–16). Nonetheless, most of these systems still require functional characterization. The peculiarities of TITAs make them difficult to study. Indeed, they are strongly regulated at the co- and post-transcriptional levels by key sequence and/or structure elements. Very often, these regulatory elements are difficult to predict and their study requires extensive genetic manipulation. Up to now, insights about TA systems from various types and bacteria were mostly gathered from studying the effects of toxin overexpression (17). Because many of these systems are chromosomally encoded, their expression should be studied at the chromosome, instead of using plasmid overexpression, to ensure studying native levels. To this end, we recently developed a strategy to study chromosomal TA expression named FASTBAC-Seq (Functional Analysis of Toxin–Antitoxin Systems in Bacteria by Deep Sequencing) (18,19). Our approach enables us to (i) assess the death-inducing capabilities of a toxin and (ii) identify single-nucleotide substitutions that abrogate the toxin's function or expression. We take advantage of the lethality induced by the expression of the toxin in the absence of the antitoxin to search for intragenic toxicity suppressor mutations. Using this method, we identified crucial elements that regulate the *aapA3*/IsoA3 TITA in *H. pylori*. In brief, we introduced mutated PCR libraries of the *aapA3*/IsoA3 and of the *aapA3*/ΔIsoA3 loci in the *H. pylori* chromosome. In the *aapA3*/ΔIsoA3 transformants, the expression of the IsoA3 antitoxin was turned off by introducing point mutations in its promoter, leading to the constitutive synthesis of AapA3 toxin and cell death. We then performed a life and death selection and identified numerous nucleotide substitutions in the CDS, but also in the UTRs impacting AapA3 protein activity or the *aapA3* toxin mRNA structure or translatability. The analysis of these mutations led to the discovery of novel regulatory elements of this system, notably the identification of functional metastable structures in the *aapA3* mRNA (18). These transient structures inhibit co-transcriptional translation of the nascent *aapA3* mRNA and prevent premature toxicity.

Here, we adapted and improved the FASTBAC-Seq method to be performed in the model organism *E. coli*, making it convenient to widely characterize TA systems from diverse types and bacteria. As a proof of concept, we investigated the well-studied plasmidic *hok*/Sok system, for which many intragenic regulatory elements have already been described and validated. Overall, we retrieved most of the already described toxicity determinants, identifying single-nucleotide mutations impeding the toxin mRNA synthesis and translation as well as the toxin activity. In particular, we detected many single-nucleotide substitutions that prevent the conformational change of the *hok* mRNA locking it in its inactive state, validating the previously published secondary structures of the FL- and Tr-*hok* mRNAs. Unexpectedly, several substitutions in the *hok* CDS were not interfering with protein activity but instead altered its expression. Overall, our method not only identified known and predicted regulatory elements, but also pointed to new ele-

ments in the CDS that act by an unknown mechanism. Delineating regulatory elements of TA is crucial to annotate these systems and develop better bioinformatic prediction tools.

MATERIALS AND METHODS

Escherichia coli strains, plasmids, oligonucleotides and culture conditions

All the *E. coli* strains used and constructed in the present study originate from the XTL632 strain 'MG1655 *galM*<*tetA-sacB*>*gpmA*' from the Court laboratory (20) and are listed in Supplementary Table S1. The plasmid and oligonucleotide sequences are listed in Supplementary Tables S2 and S3. *Escherichia coli* strains were grown on LB agar plates (Condalab) and in LB broth (Condalab) (with 30 μg/ml chloramphenicol when needed).

hok/Sok cassettes inserted in *E. coli*

The studied locus *hok*/Sok originates from the *E. coli* plasmid R1 minimal *parB*⁺ region (sequence corresponding to entry TA07123 in T1TADB: <https://d-lab.arna.cnrs.fr/t1tadb>, from NCBI GenBank accession number X05813). The sequences of *hok*/Sok, *hok*/ΔpSok (containing point mutations inactivating Sok promoter) and Δ*phok*/ΔpSok (containing point mutations inactivating both *hok* and Sok promoters) were synthesized (IDT-DNA, gBlocks, Supplementary Table S4) and inserted in *E. coli* by λ-red recombination following the protocol from the Court laboratory (21) and summarized below. The strain XTL632 'MG1655 *galM*<*tetA-sacB*>*gpmA*' was used as a recipient strain and its *tetA-sacB* cassette was replaced by the different wild-type (WT) and mutated *hok*/Sok cassettes. Note that the XTL632 strain contains five endogenous *hok*/Sok systems, namely *hokA*, *hokB*, *hokC*, *hokD* and *hokE* (3).

FASTBAC-Seq experiment

The synthesized DNA sequences *hok*/Sok, *hok*/ΔpSok and Δ*phok*/ΔpSok were first amplified by three cycles of PCR with FA890 and FA891 using the Phusion High-Fidelity Hot Start DNA Polymerase (Thermo Fisher Scientific) to add the flanking regions necessary for recombination at the *tetA-sacB* site in *E. coli*, and then by 30 cycles of PCR with FA873 and FA874 using the Dream Taq DNA polymerase (Thermo Fisher Scientific) introducing mutations in the PCR fragments. After purification using the 'gel extraction kit' (Neobiotech), these PCR products were introduced in *E. coli* by electroporation. In brief, after an overnight culture with 50 μg/ml of hygromycin at 30°C, 180 rpm, the XTL632 strain was diluted 70-fold in fresh medium and grown during 2 h at 32°C (to reach 0.4 < OD_{600nm} < 0.6) without antibiotics. Induction of the λ-red recombination functions was performed by heat shock at 42°C for 15 min. The cells were rendered competent using ice-cold water and 50 μl of competent cells were mixed with either 10 μl of 10 ng/μl PCR fragments (100 ng total) or H₂O for the negative control, and electroporated at 1.8 kV in 0.1 cm cuvettes (Dutscher). The cells were recovered after 4 h at

32°C, 180 rpm, in 10 ml of LB medium, before being pelleted, washed with M9 medium and plated on ‘Tet/SacB counter-selection plates’ [prepared as described in (21): 4 g tryptone, 4 g yeast extract, 15 g Difco agar, 8 g NaCl, 8 g NaH₂PO₄·H₂O, 100 ml of a 60% sucrose stock solution, 0.5 ml of a 48 mg/ml fusaric acid (Sigma) stock solution in ethanol, 32 ml of a 25 mM ZnCl₂ stock solution) at 42°C. The total viable cells were determined by plating 50 µl of a 10⁻⁶ dilution in triplicate on LB agar plates. Ninety-six transformants from the ‘Tet/SacB plates’ were tested by colony PCR using FA873 and FA874, and the PCR products were sequenced. All the transformants tested had integrated the *hok/Sok* cassette. *Escherichia coli* strains with *hok/Sok* and Δ *phok*/ Δ pSok were checked for sequence integrity and frozen as EFD475 and EFD515, respectively. Insertion of the *hok*/ Δ pSok was toxic and resulted only in transformants with mutations in the locus; individual mutants were frozen (Supplementary Table S1). This experiment (both PCR and transformations) was repeated five times independently and we retrieved from 3000 to 15 000 colonies (same number per experiment, according to the smallest number obtained). The genomic DNA of the mixture of colonies was extracted using the Quick Bacteria Genomic DNA Extraction Kit (Neobiotec) following the supplier’s recommendations. The *hok/Sok* locus was amplified by FA910 and FA911 (carrying Illumina adapters) using the Mix 2X KAPA HiFi HotStart (Roche), resulting in 486 nucleotide (nt) amplicons. The amplicons were sequenced at the Bordeaux Transcriptome Genome Platform (Cestas-Pierroton, France) by Illumina technology on a MiSeq V3 instrument in paired-end mode (2 × 300 nt with overlapping reads).

FASTBAC-Seq data analysis

Sequence data were processed and analyzed as in (19) with slight adjustments [software versions and parameters that differ from (19) are given below]. The numbers of total reads, merged reads and mapped reads are available in Supplementary Table S5. Briefly, the analysis pipeline included the following steps for each sample: (i) trimming low-quality 3’ ends of reads and discarding low-quality reads using cutadapt (<https://cutadapt.readthedocs.io/en/stable/>) and prinseq-lite (22); reverse reads (R2 reads) were also trimmed of their first seven bases (option ‘-trim_left 7’ in prinseq-lite) because there was a large proportion (>20%) of these reads with undefined bases in this region; (ii) recovering read pairs for which both mates passed the quality filtering steps using cmpfastq (https://github.com/iirisarri/scripts_main/blob/master/cmpfastq.pl) and assembling mates into a single sequence by means of PANDAseq 2.9 (23) run with options ‘-N -o 20 -O 0 -t 0.6 -A simple_bayesian -C empty’; (iii) aligning these assembled reads onto the 486 nt reference sequence (*hok/Sok*, *hok*/ Δ pSok or Δ *phok*/ Δ pSok sequence, depending on the sample) by the BWA-MEM algorithm of BWA 0.7.17 (24) run with options ‘-A 1 -B 4 -O 6 -E 1 -L 10, 10’; (iv) extracting mapped sequences of length 486 nt and showing a single-nucleotide substitution compared to the reference using samtools 1.9 (25) and bamtools (<https://github.com/pezmaster31/bamtools>); and (v) performing statistical analyses of the

differential distribution of single-nucleotide mutations between *hok/Sok* or Δ *phok*/ Δ pSok and *hok*/ Δ pSok sequences. For substitutions, a ‘nucleotide-specific’ analysis to determine whether particular nucleotides were enriched at specific positions was carried out exactly as described in (19) using Trinity 2.10.0 (19,26), R 3.5.3 (<https://www.R-project.org/>) and DESeq2 1.22.2 (27). Mutations were considered as significantly over- or under-represented in the mutant versus the reference sample if the adjusted *P*-value (*P*_{adj}, corresponding to the false discovery rate) was inferior or equal to 5% (*P*_{adj} ≤ 0.05) and the log₂ fold change (FC) was superior or equal to 1 or inferior or equal to -1 (|log₂ FC| ≥ 1) (Supplementary Table S6). We then combined the results of the differential distribution of mutations in *hok/Sok* versus *hok*/ Δ pSok and Δ *phok*/ Δ pSok versus *hok*/ Δ pSok (Supplementary Table S6). Note that the positions corresponding to the mutated nucleotides of *hok* or *Sok* promoters were not included in the analysis. Three positions had a negative log₂ FC, meaning that they were more frequent in *hok/Sok* or Δ *phok*/ Δ pSok than in *hok*/ Δ pSok and were not further studied.

Construction of plasmids expressing *hok*-FLAG variants

The synthesized DNA sequence *hok*/ Δ pSok was amplified by FB64/FB66 and FB67/FB65 primer pairs to add the FLAG sequence and the two fragments were then assembled using FB64/FB65. The resulting fragment was cloned in pAZ3 digested with EcoRI and HindIII to generate the plasmid pEFD558, which was used as a template to construct the plasmids carrying mutated Hok* -FLAG variants. The mutations were introduced with a two-step PCR, using primers listed in Supplementary Table S3. The sequence integrity of all obtained plasmids was checked using FA858.

Total RNA extraction

Six hundred twenty-five microliters of Stop Solution (95% ethanol, 5% phenol, pH 4.5, 4°C) was added to 5 ml of exponentially growing cultures. The cells were immediately centrifuged and the pellets were stored at -80°C. After resuspension in 400 µl Lysis Solution (20 mM NaAc, pH 5.2, 0.1% SDS, 1 mM EDTA), the samples were transferred into 400 µl hot phenol (pH 5.2) and incubated for 10 min at 65°C. The samples were centrifuged for 10 min at 13 000 rpm at room temperature and the aqueous phase was transferred to a phase-locked gel tube (Eppendorf) containing an equal volume of chloroform/isoamyl alcohol. After 10 min of centrifugation at 13 000 rpm at room temperature, the aqueous phase was mixed with 2.5 volumes of 100% ethanol and 0.1 volume of 3 M NaAc (pH 5.2) and incubated overnight at -20°C. The precipitated RNAs were centrifuged for 30 min at 13 000 rpm at 4°C, washed with 70% ethanol, air-dried and resuspended in H₂O. The RNA concentration was determined using a DeNovix and the RNA integrity was checked on 2% agarose gel stained with EtBr.

Northern blot

Ten micrograms of total RNA was separated on 8% polyacrylamide/7 M urea gels in 1 × Tris–borate–EDTA

(TBE). The RNAs were transferred to a Nylon membrane (Hybond-N, GE Healthcare Life Sciences) by electroblotting in 1 × TBE at 8 V and 4°C overnight and cross-linked to the membrane by UV irradiation (302 nm) for 2 min in a UV cross-linker. The FB178, FA909, FB181 and FD211 (5S) oligonucleotides (Supplementary Table S3) were labeled at their 5' end with ³²P and incubated with the membranes in a modified Church Buffer (1 mM EDTA, 0.5 M NaPO₄, pH 7.2, 7% SDS) overnight at 42°C. The membranes were washed two times for 5 min in 2 × SSC and 0.1% SDS and revealed using a Pharos FX phosphorimager (Bio-Rad).

Western blot

Cell pellets from 1 ml culture reaching OD_{600nm} between 0.5 and 0.8 were lysed in Lane Marker Reducing Sample Buffer 1 × (Thermo Scientific) (100 μl for 1 OD₆₀₀/ml) incubated at room temperature in an ultrasound water bath for 15 min. Samples were incubated with 25 units of Benzonase (Merck) at room temperature for 15 min. Ten microliters of each sample was separated on 16% SDS-PAGE gels (1 M Tris, pH 8.45, glycerol 10%, 0.1% SDS) in cathode buffer (0.1 M Tris, 0.1 M tricine, 0.1% SDS) and anode buffer (0.1 M Tris-HCl, pH 8.9) at 60 V for 30 min and at 160 V for 90 min. Proteins were transferred to a nitrocellulose membrane in transfer buffer (Tris-glycine 1 ×, ethanol 20%, SDS 0.05%) at 90 V for 90 min. The membrane with total proteins was stained with SYPRO™ Ruby Protein Gel Stain (Thermo Fisher Scientific) and detected using a Pharos FX phosphorimager (Bio-Rad). Membranes were blocked with 5% skimmed milk in TBS 1 × and Tween 20 0.5%, then incubated with 1:800 monoclonal anti-FLAG M2 and 1:10 000 anti-rabbit IgG (whole molecule)-peroxidase (Sigma) and revealed using Western Clarity ECL (Bio-Rad) on a Chemidoc (Bio-Rad).

RESULTS AND DISCUSSION

Experimental strategy and application to the *hok/Sok* TITA system

TITA systems are small toxic genetic modules whose expression involves multiple levels of co- and post-transcriptional regulations (2). We recently developed the FASTBAC-Seq method, which is a powerful tool to quickly reveal key regulatory elements. The aim of the present study was to establish this method in the model organism *E. coli*. Indeed, the original method could only be carried out in the human gastric pathogen *H. pylori* (18,19), which hampered the analysis of multiple predicted TA systems.

Before going to the detailed study of the *hok/Sok* system, here is a brief summary of our revised experimental strategy summarized in three steps. (I) The first step is to generate mutated PCR libraries of TA and Δantitoxin (ΔA) loci from synthesized DNA fragments (Figure 1). In the ΔA fragment, the promoter of the antitoxin is lacking or inactivated by point mutations. It is essential to check that the mutations in the antitoxin promoter are effectively abrogating antitoxin expression, for instance, by using northern blot. (II) Then, these PCR libraries are transformed in *E. coli* and integrated by homologous recombination in a chromosomal region of interest containing a selection/counter-

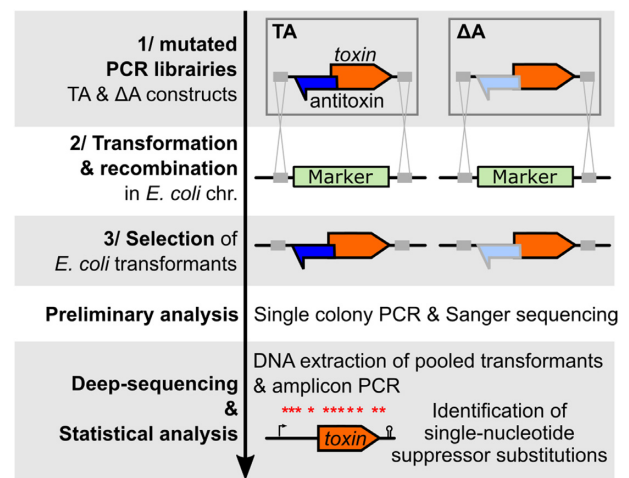


Figure 1. Strategy of FASTBAC-Seq in *Escherichia coli*. (1) The first step is to generate mutated PCR libraries from TA and ΔA sequences containing flanking regions (gray boxes) allowing recombination in the *E. coli* chromosome. To do this, chemically synthesized DNA fragments (TA and ΔA) are amplified using the Taq polymerase, generating mutations. The gray outline and lighter blue color of the antitoxin in the ΔA construct indicates the loss of expression due to point mutations in the promoter. (2) The PCR libraries are then introduced in an *E. coli* recipient strain containing a selection/counter-selection marker (in green) and (3) transformants are selected on appropriate media. Preliminary analysis: The TA and ΔA constructs of randomly chosen transformants are amplified and sequenced. If the TA loci of all ΔA transformants are mutated, it indicates that mutations are necessary for survival and therefore the expression of the toxin from the *E. coli* chromosome is toxic in the absence of the antitoxin. In contrast, only a proportion of TA should be mutated. Deep-sequencing & Statistical analysis: Several independent PCR reactions for each PCR library are transformed and integrated in the *E. coli* chromosome. All the colonies obtained from the same transformation are pooled together and the TA and ΔA loci are amplified by PCR after DNA extraction. The amplicon is sequenced using Illumina technology and mapped against the WT sequence, and the occurrence of single-nucleotide substitutions is compared between the TA and ΔA using statistical analysis. The substitutions significantly enriched in the ΔA relative to TA samples are annotated as loss-of-function substitutions, mapped over the TA locus and further studied.

selection cassette. (III) Finally, the transformants are selected by the loss of the cassette and first analyzed by single colony PCR and Sanger sequencing. Because this method is designed for the study of death-inducing toxins, it is crucial to demonstrate the toxicity of the studied toxin when expressed from the chromosome. This is easily assessed by individually sequencing several ΔA transformants (Figure 1). If all surviving colonies contain inactivating mutations, it indicates that the ΔA construct is toxic. Once the toxicity is confirmed, loss-of-function mutants can be identified in a high-throughput manner. All transformants obtained from each biological replicate are pooled together and steps of DNA extraction, amplicon PCR and deep sequencing are performed (Figure 1). Finally, the mutants of interest can be reconstructed individually to validate their ability to grow and assess their effect on transcription and translation using routine molecular techniques.

To set up our new protocol, we chose the best characterized TITA of *E. coli*, the *hok/Sok* system discovered on the R1 plasmid (5). We first designed three *hok/Sok* constructs to be integrated in the *E. coli* chromosome, namely

the *hok*/Sok toxin–antitoxin (HS), *hok*/Δ*pSok* (HΔS), but also Δ*phok*/Δ*pSok* (ΔHΔS) as an additional control (Figure 2A). In the HS locus, both the toxin and antitoxin RNAs are expressed and the antitoxin binds to the Tr-*hok* mRNA leading to its degradation. In HΔS, only the toxin RNA is expressed, as the transcription of the Sok antitoxin is turned off by mutations in its promoter region. The Hok protein should be produced in this construction. In ΔHΔS, the transcription of both the *hok* toxin mRNA and the Sok antitoxin RNA is inhibited by mutations in their respective promoters.

We first amplified the three synthesized DNA fragments by PCR using a low-fidelity Taq DNA polymerase introducing mutations (Figure 1). The PCR libraries were then transformed in *E. coli* XTL632, a strain harboring a *tetA-sacB* selection/counter-selection cassette in its chromosome between the *galM* and *gpmA* genes (20) (Supplementary Figure S1). The *tetA* gene confers tetracycline resistance and fusaric acid sensitivity, while *sacB* confers sucrose sensitivity. We promoted *E. coli* recombination functions following a robust protocol (21). Briefly, we induced the expression of the λ-red recombination genes from the pSIM18 plasmid before preparing electrocompetent cells and transforming the constructs of interest by electroporation. We then selected the transformants in which the *tetA-sacB* selection cassette was replaced by the HS, HΔS or ΔHΔS constructs by plating on LB agar containing fusaric acid and sucrose (21) (Supplementary Figure S1). All the clones tested individually had integrated the constructs, confirming that this selection method was highly efficient.

Preliminary analysis: chromosomal expression of Hok is toxic

We sequenced two transformants for the HS and ΔHΔS PCR transformations, as well as 91 transformants for HΔS. As expected, we obtained unmutated sequences for HS and ΔHΔS; however, all HΔS colonies carried loss-of-function mutations in their locus (HΔS). Among them, we obtained 26 clones with a single-nucleotide substitution, 22 clones with a single deletion and the 43 other clones containing more complex mutations (one or several truncations, and several substitutions/deletions/insertions) (Supplementary Table S6). Two mutations were located in the *hok* promoter, one in the *mok* start codon and two led to a premature stop codon in *hok*. This demonstrated that the expression of a chromosomal copy of *hok* from the R1 plasmid using its native promoter is toxic for *E. coli* in the absence of the Sok antitoxin. Hok was previously shown to be toxic when expressed from a plasmid but never from the chromosome. Therefore, our work reveals that the level of chromosomal expression is not the limiting factor for these systems to be active. In addition, the five endogenous chromosomal *hok* systems were not deleted in the strain used in this study, showing that none of the chromosomal Sok RNAs could inhibit the expression of the studied *hok*.

As a first approach to understand the suppression mechanism of some of the substitutions, we inspected *hok* and Sok RNA expression by northern blot analysis (Figure 3A). As expected from previous studies, we observed the Sok

RNA and two isoforms of the *hok* mRNA for the WT locus. Those two bands correspond to the FL inactive forms of the *hok* mRNA in which the SD of *mok* is sequestered, impeding *hok* translation (10). The Tr-*hok* mRNA is absent in the WT as it is degraded together with the Sok antitoxin by RNase III (10). In ΔHΔS transformants, both the *hok* and Sok RNAs were absent validating that the mutations in the promoters inhibit transcription, as expected. In the various HΔS mutants, Sok was absent and the pattern of *hok* expression varied between the mutants. In addition to both FL-*hok* mRNAs, the translatable Tr-*hok* mRNA was present in most mutants indicating that these mutations impair Hok translation or activity. In the mutants located in the 3' UTR (G345A and C358A), the Tr-*hok* mRNA was absent, preventing toxicity by destabilizing or inhibiting the production of this active form. To further understand the mechanism of loss of function, we constructed plasmids expressing selected Hok mutants tagged with a C-terminal FLAG (inhibiting toxicity) under arabinose induction. The mutated Hok (Hok^{*}) protein production was then monitored by Western blotting analysis (Figure 3B). We observed extremely different patterns of Hok^{*} expression although the mutated *hok* mRNAs were comparably expressed (Supplementary Figure S2). These results suggest that some of the mutations inhibit translation (e.g. A106G) while other interfere with Hok toxin activity (T204T and G311T).

High-throughput analysis and overview of the results

The results described above showed that our transformation and selection method was efficient and suggested that it was suitable for discovering single-nucleotide suppressor mutants in a high-throughput manner. For this, we scaled up our analysis and prepared five biological replicates of each PCR sample (HS, HΔS, ΔHΔS). We pooled the transformants, extracted the DNA, amplified the locus by PCR and submitted our samples to deep sequencing. After assembling read pairs, we obtained 2.3 million reads of exactly 486 nt mapped to the amplicon for the HS, 1 million for HΔS and 1.8 million for ΔHΔS (Supplementary Table S5). About 30% of the reads were not mutated in the HS and ΔHΔS and around 15% were not mutated in HΔS. Considering the deadly phenotype of unmutated HΔS, the high proportion of unmutated sequences in these reads probably corresponds to amplification of dead cell DNA. One could consider replicating the transformants on a fresh plate before pooling the cells for DNA extraction to avoid this noise in the sequencing data.

To identify loss-of-function single-nucleotide substitutions, we retrieved all reads having only one substitution and performed differential distribution analysis between HS or ΔHΔS and HΔS sequences at each position of the amplicon for each possible nucleotide. The mutations were well distributed over the amplicon (Fig 2B), unlike in our previous study in *H. pylori* where a disproportionate peak of mutations was found at the PCR overlap region. In total, 162 single-nucleotide substitutions were statistically significantly enriched in the HΔS samples compared to the HS and ΔHΔS controls, located in 117 positions throughout the 486 nt amplicon (Supplementary Table S6). This in-

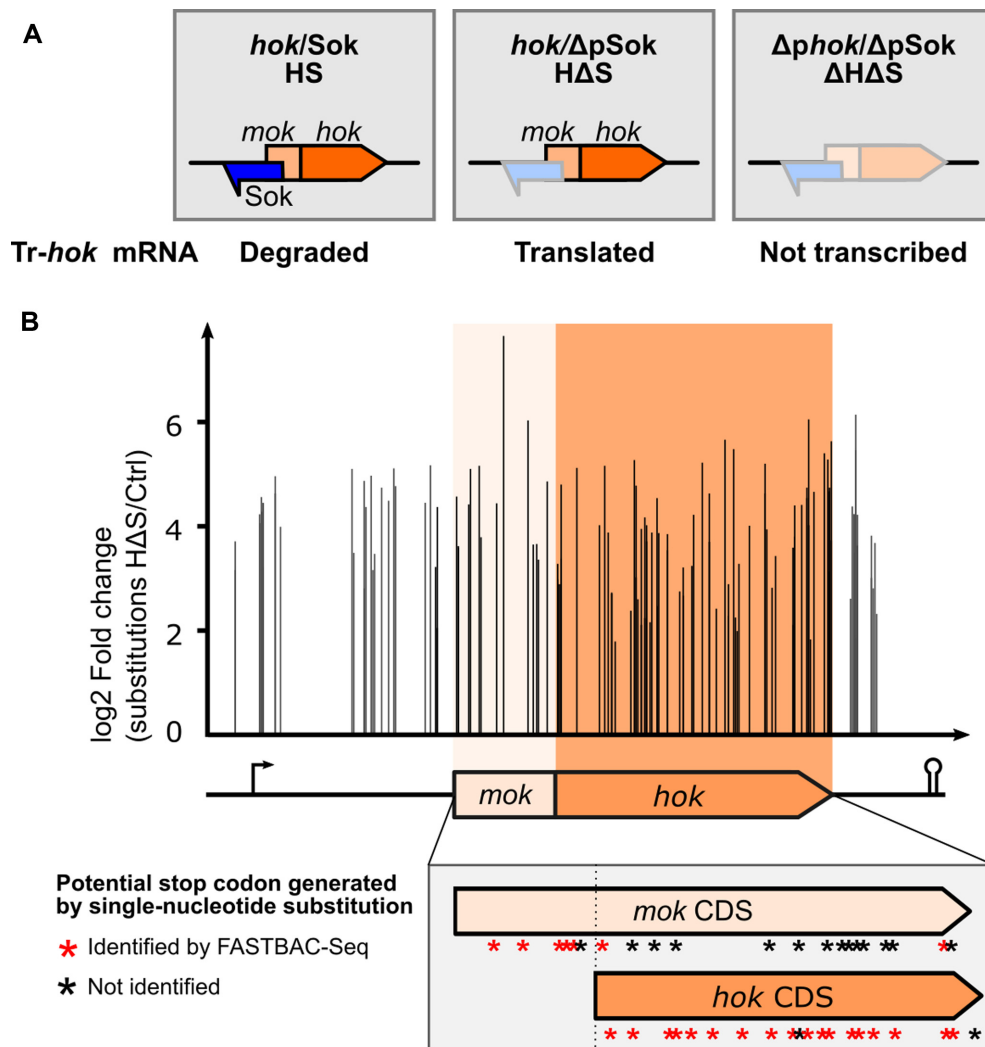


Figure 2. Identification of single-nucleotide suppressor substitutions in the *hok/Sok* locus. (A) The *hok/Sok* locus consists of two overlapping CDSs, the leader peptide *mok* and the toxic protein *hok*, and of the *Sok* noncoding RNA. The *mok.hok* mRNA (or *hok* mRNA) is transcribed as an untranslatable FL mRNA that is processed at the 3' end to form a translatable, truncated mRNA (Tr-*hok*). Here, the HS, HΔS and ΔHΔS constructs were amplified by FASTBAC-Seq and individually introduced into the *E. coli* chromosome. The expected expression of each of the three constructs designed for FASTBAC-Seq is indicated. HS: The *Sok* antitoxin inhibits the Tr-*hok* mRNA translation by inducing degradation of the toxin/antitoxin RNA duplex by RNase III. HΔS: In the absence of the *Sok* antitoxin, Tr-*hok* mRNA can be translated and is toxic for the host cell. ΔHΔS: The locus with the promoters of both *hok* and *Sok* inactivated was used as a control; *hok* and *Sok* are not transcribed. (B) FASTBAC-Seq results. The differential distribution of single-nucleotide substitutions was statistically analyzed between the *hok*^{*}/Δp*Sok* and the controls (ctrl) *hok/Sok* and Δ*hok*/Δp*Sok*. We obtained loss-of-function substitutions (occurring statistically more in *hok*^{*}/Δp*Sok*) well distributed over the *hok/Sok* locus. The arrow represents the promoter, and the 'stem-loop' represents the terminator. The CDSs of *mok* and *hok* are shown in orange colors. The zoomed gray box shows the location substitution leading to stop codons in *mok* or *hok* CDS.

cluded 128 single-nucleotide substitutions enriched in both comparisons and 34 additional substitutions identified only in one comparison, 17 in the HS versus HΔS and 17 in the ΔHΔS versus HΔS comparison. The fact that 79% of the substitutions were found in both conditions and that we retrieved all the substitutions identified during the preliminary analysis validated the strength of our study. To be fully exhaustive, we retained all significant substitutions, including the ones found in one comparison only.

Among the 162 total substitutions identified, 79 positions were substituted with only 1 nt, 31 with 2 nt and 7 with the 3 possible nt. In total, 2 substitutions mapped in the *hok* promoter, 31 in the *hok* mRNA 5' UTR (upstream of the *mok* CDS), 20 in the *mok* CDS (upstream of the *hok* start

codon), 87 in the *hok* CDS and 22 in the *hok* mRNA 3' UTR (Figure 2B, Table 1, Supplementary Table S6).

Validation of the method: suppressor mutations in promoter and coding sequences

We validated many well-known determinants of *hok/Sok* regulation such as the promoter and the *hok* CDS. We could locate the toxin mRNA promoter sequence and identified the precise nucleotides required for its functionality. Indeed, we obtained four substitutions in the -10 box promoter sequence (TATGAT) of the *hok* gene, two from the deep sequencing analysis (A-11C/G) and two from the preliminary analysis (T-12C and T-7C). This is consistent with

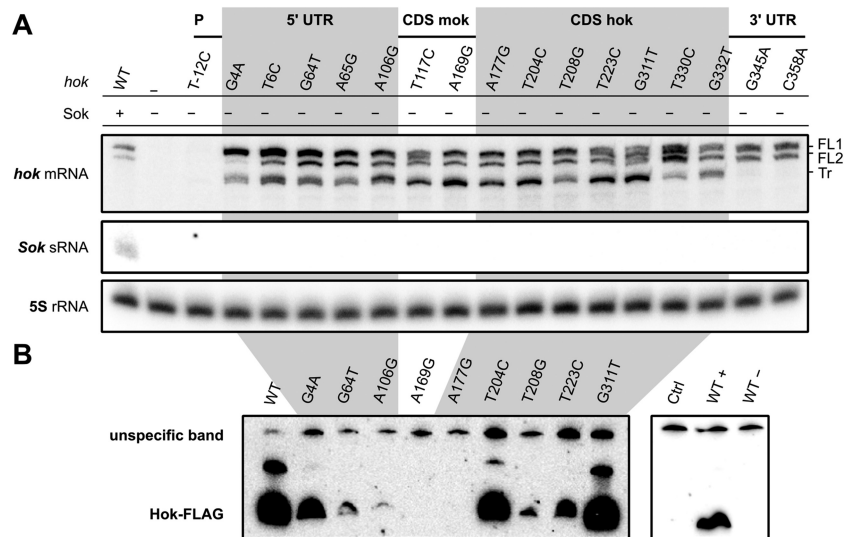


Figure 3. Characterization of *hok* suppressor substitutions. (A) Northern blot analysis of *hok* and Sok RNAs. The *hok* mRNA was revealed using a probe matching the *hok* mRNA 5' UTR (FB178). The two FL forms of WT *hok* mRNA were detected in all transformants expressing *hok*. The translatable Tr-*hok* mRNA was present in most mutants, except for C345A and C358A. Sok was targeted with the probe FB213 and was absent in H⁺ΔS strains. 5S rRNA was revealed using probe FD211 and used as a loading control. P: promoter. (B) Western blotting of arabinose-induced Hok-FLAG protein mutants from pBAD plasmids (*hok**-FLAG mRNA expression is stable; see Supplementary Figure S2). The upper signal corresponds to an unspecific band, as confirmed with pBAD vector control as well as induced (WT+) and uninduced (WT-) WT Hok-FLAG.

Table 1. Summary of the localizations of single-nucleotide loss-of-function substitutions identified

Location of the substitutions	Number of substitutions (number of positions)	Predicted mechanism of action
Promoter	2 (1)	Transcription inhibition
<i>hok</i> mRNA 5' UTR	31 (22) 10 (4) 7 (7) 2 (2) 12 (9)	Destabilization of the tac-stem Stabilization of aSD pairing Mutation of <i>mok</i> SD sequence Unknown
<i>mok</i> CDS	20 (18) 4 (2) 5 (5) 11 (11)	Mok and Hok not translated Mok truncated and Hok not translated Unknown
<i>hok</i> CDS	87 (64) 81 (59) 3 (2) 3 (3)	Hok activity impaired Hok not translated Unknown
<i>hok</i> mRNA 3' UTR	22 (12) 19 (9) 3 (3)	Degradation by RNase Unknown

The locations of all significant substitutions obtained by FASTBAC-Seq are indicated as well as their number, and the number of nucleotide positions mutated is given in parentheses. The predicted mechanism of action for those mutations is indicated. See Supplementary Table S6 for details. CDS: coding sequence.

the conserved TANNNT (where N means any nucleotide) –10 box promoter sequence described for *E. coli* (28). We also confirmed that the *hok*_{T-12C} mutant was not transcribed in this strain (Figure 3A).

We next examined the 87 substitutions in the *hok* CDS. As expected, we obtained substitutions impairing Hok production and activity, located in the start (3) and stop codons (6) as well as mutations leading to a premature stop codon (18) and nonsynonymous amino acid changes (57) (Figure 2B, listed in Supplementary Table S6, Supplementary Fig-

ure S3). Unexpectedly, we also obtained three synonymous substitutions preserving the *hok* amino acid sequence.

The *hok* start codon was mutated on its second and third positions. As expected, substitution of the start codon from AUG to GUG/UUG/CUG was not observed as those codons all constitute valid alternative start options for translation (29). Six substitutions abrogated the *hok* stop codon, leading to the formation of a 17-aa longer protein. It is expected that these proteins are not toxic, as adding a C-terminal 8-aa FLAG-tag entails loss of toxicity. Indeed,

in two of these mutants (T330C and G332T) the Tr-*hok* mRNA is present and may be translated (Figure 3A).

We monitored the abundance of the Hok*–FLAG mutants carrying nonsynonymous mutations, postulating that they should be expressed at a similar level to the WT Hok-FLAG protein. While the T204C_{C11R} (T204C corresponds to amino acid substitution C11R) and G311T_{M46I} mutants produced Hok protein levels comparable to the WT, T208G_{V12G} and T223C_{L17P} produced less Hok and Hok from A177G_{K2E} was not detected (Figure 3B). Note that the *hok* mRNA was present at a comparable level in all those strains (Supplementary Figure S2). This unexpected result strongly suggested that not all CDS substitutions lead to the production of inactive Hok proteins, but some can also affect translation, Hok protein stability or Hok mRNA stability (although we did not have any example among the mutants tested by northern blot). Finally, the mechanism of action of the substitutions in the *hok* CDS leading to synonymous substitutions (A227U_{T18T}, A320G_{E49E} and U326C_{G52G}) remains to be understood. These mutations may act at the structural level, as demonstrated for a synonymous substitution observed in the FASTBAC-Seq analysis of the *aapA3* locus of *H. pylori* (18).

Translational regulation by the *mok* leader peptide

The start codon of the 70-aa *mok* leader peptide was affected by four substitutions T117C, T117G, G118T and G118A (Supplementary Table S6), validating that Mok translation is required for Hok translation. The presence of the Tr-*hok* mRNA in the T117C clone was consistent with the absence of translation (Figure 3A).

It was known that inserting a stop codon in *mok* after the *hok* start codon does not have any effect on *hok* translation. Therefore, it was proposed that only translation of *mok* up to *hok* translation initiation region is important to start *hok* translation (6). To test this, we tallied up the number of stop codons that could theoretically be generated by single-nucleotide substitutions in *mok* and *hok* and compared it with the actual number identified here. We obtained 18 out of the 20 codons from *hok* that could be theoretically changed to a stop codon by only one substitution and 7 out of 21 for *mok*, including 5 upstream of the *hok* start codon and only 2 downstream (Figure 2B, Supplementary Figure S3). Our data support that translation of the *mok* mRNA at least up to the *hok* SD is mandatory to allow Hok translation and that *mok* translation beyond the *hok* start codon is not necessary for *hok* to be translated. The two substitutions identified downstream of the *hok* start codon (G176T and T315A) inhibit toxicity likely by affecting the *hok* and not the *mok* CDS (mutation of the *hok* start codon and production of Hok_{Y48N}).

Thus, we analyzed the 20 substitutions identified in the 19 first amino acids of *mok* (located upstream the *hok* start codon). In addition to the four substitutions in *mok* start codon and the five premature stop codons, we identified six nonsynonymous and five synonymous changes in Mok. Amino acid substitutions in Mok should not affect Hok production (6); therefore, we hypothesize that these mutations affect the translatability of *hok* via other mechanisms such as interfering with sequences important for

translation or affecting the toxin mRNA structure. Substitutions A163G_{G16G}, A159G_{Q15R}, A159G_{Q15Q}, A166G_{E17E} and A169G_{E18E} are in the close vicinity of the *hok* SD sequence and could affect SD recognition. The pattern of expression of *hok* was tested in the Hok_{A169G_{E18E}} synonymous mutant. The Tr-*hok* mRNA was observed; however, the flagged protein was not translated (Figure 3B). Future experiments will be required to understand the exact mechanism of action of these mutations.

Deciphering functional determinants of the *hok* mRNA structure

We obtained 31 substitutions in the *hok* mRNA 5' UTR (upstream of the *mok* start codon) and 22 substitutions in the 3' UTR. These substitutions could affect either specific sequences guiding translation, like the *mok* SD, or the structure of the translatable Tr-*hok* mRNA (18). Indeed, the *hok* 5' UTR adopts a closed conformation in the FL-*hok* mRNA but also in the nascent *hok* mRNA, where a metastable structure is formed, and an open conformation in the Tr-*hok* (8). The *hok* mRNA is not translatable when it adopts the closed conformation since the *mok* SD is sequestered in a stem-loop structure via pairing with the aSD (anti-SD or ucb). However, in the open conformation of the Tr-*hok* mRNA, the *mok* aSD is trapped by the tac-stem structure rendering the mRNA translatable (Figure 4A, Supplementary Figure S4).

We identified three mutations in the GAGG *mok* SD motif: G105T and A106G/T. While the G105T and A106T substitutions (Supplementary Figure S4, dark blue) likely impair the base pairing with the 16S rRNA SD complementary sequence, this should not be the case for the A106G substitution, which allows the formation of a GU wobble pair. In contrast, the A106G substitution strengthens the *mok* SD/aSD interaction by creating an extra base pair (Figure 4B, green box). Since the Tr-*hok* mRNA form was observed in this strain (Figure 3A), we hypothesize that the increased stability of the SD/aSD interaction prevents the conformational change and locks the truncated form in the closed conformation, thereby inhibiting the translation of *mok*, and consequently that of *hok*. Indeed, we monitored the abundance of Hok*_{A106G}-FLAG by Western blot and observed a very strong inhibition of Hok translation (Figure 3B). Strengthening this hypothesis, we found that the C74T substitution located in the *mok* aSD and opposite to A106G in the FL-*hok* mRNA conformation was also responsible for loss of function. Five additional substitutions could have the same mechanism of action (Figure 4B, green box).

We also found substitutions affecting the nucleotides G4, C5 and T6 (Figure 4B, purple box). For each of these nucleotides, a substitution into the three other possible nucleotides abolished *hok* toxicity, implying that those mutations act by breaking base pairs. These substitutions could be disturbing the formation of the open tac-stem structure as they base-paired with the ucb *mok* aSD sequence in the FL-*hok* mRNA. Both the FL- and the Tr-*hok* mRNA forms were present in the northern blot analyses of G4A and T6C, and the abundance of Hok*_{G4A}-FLAG was drastically reduced compared to the WT, validating the effect on Hok

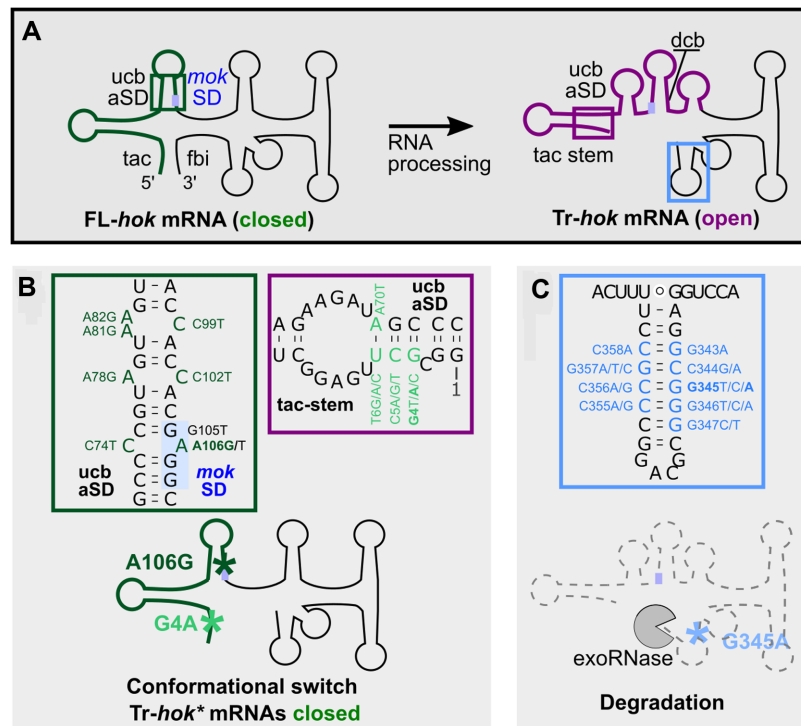


Figure 4. Single-nucleotide substitutions affect *hok* mRNA structural conformation and stability. (A) *hok* mRNA is transcribed and folded into a FL isoform with a closed conformation [*mok* SD (blue box) sequestered] that is not translatable. Following maturation by RNase(s), a translatable Tr-*hok* mRNA form with an open conformation is produced. In the WT, this form is targeted by Sok, whereas in the absence of Sok, Hok is produced entailing bacterial cell death. tac: translational activator element; fbi: fold-back inhibitory element; ucb: upstream complementary box; dcb: downstream complementary box. The schematic structures are based on (8). (B) Several substitutions prevent the conformational change of Tr-*hok* mRNA from the closed to the open form, locking the *hok** mRNA in the closed, untranslatable form with *mok* SD sequestered even after processing. Those substitutions act by either stabilizing the closed structure (green box) or destabilizing the open structure (purple box). Green box: Seven single substitutions (dark green, including A106G) increased the stability of the *mok* SD/aSD stem-loop by creating extra base pairs locking Tr-*hok* mRNA in the closed conformation. Purple box: Ten single substitutions (four positions, light green including G4A) decreased the stability of the tac-stem-loop in the open conformation by disrupting base pairs. (C) Blue box: Nineteen substitutions (nine positions) affected negatively the stability of the last stem-loop at the 3' end of Tr-*hok* mRNA (blue), therefore increasing its susceptibility to 3'-to-5' exoRNases. See also Supplementary Figure S4.

translation (Figure 3). We concluded that these mutations could prevent Tr-*hok* mRNA translation once again by preventing a conformational change between the FL- and the Tr-*hok* mRNA, this time by destabilizing the Tr-*hok* mRNA conformation. In addition, we identified a mutation opposite to T6 in the tac-stem, A70T (located in the *mok* aSD), which is also responsible for a loss of function. Substitutions of G71 and C72, which are also part of the *mok* aSD, were not retrieved in our analysis, suggesting their importance for the sequestration of the *mok* SD in the FL mRNA. Indeed, a mutation in those two positions would release the *mok* SD and allow Hok translation before even affecting the tac-stem formation.

Overall, the mutations in the *hok* mRNA 5' UTR locking the toxin mRNA in an inactive conformation for translation initiation are reminiscent of loss-of-function mutations identified in *aapA3* mRNA of *H. pylori* (18). These mutations acted at the mRNA folding level to trap transient structures in an untranslatable state.

Other mutations of the *hok* 5' UTR led to loss of function but, based on our current knowledge of the mRNA conformation, we were not able to propose any possible mechanism of action. For example, in the G64T mutant, the Tr-*hok* mRNA was present and the abundance of the Hok pro-

tein was drastically reduced compared to the WT explaining its lack of toxicity (Figure 3, Supplementary Figure S4, red).

We obtained 22 substitutions in the *hok* mRNA 3' UTR, among which 19 broke a CG pair in the terminal stem of the Tr-*hok* mRNA (including G345A and C358A). We observed that the Tr-*hok* mRNA form was absent in the G345A and C358A mutants (Figure 3A) showing that weakening the 3' stem-loop affects the overall *hok* mRNA stability. This effect is probably due to the action of 3'-to-5' exoRNases such as PNPase, as previously proposed (10) (Figure 4C, blue box).

Further considerations and possible limitations of the method

Although our method is a powerful tool to rapidly identify loss-of-function mutations and characterize TITAs, a few considerations and limitations should be taken into account.

First, among the 20 codons from *hok* that could be theoretically changed to a stop codon by only one substitution, only 18 were mutated (Figure 2B, listed in Supplementary Table S6). In addition, 20% of the substitutions that we obtained were only found in comparing HΔS with HS or with

$\Delta H\Delta S$ (10% in each). Altogether, these observations suggest that we might not have identified all loss-of-function mutants, probably because we did not collect enough transformants to avoid false negatives.

Second, mutations affecting the previously studied mechanism of *hok* regulation (conformational changes and stabilization of the untranslatable structure) have been smoothly annotated thanks to the fact that the *hok* mRNA structure was already well characterized. We recommend, when investigating an mRNA whose structure is unknown, to perform computational folding using alignment of homologous sequences in parallel to FASTBAC-Seq to facilitate the interpretation of the results (8,30–31). However, even with good knowledge of the mRNA structure, we also obtained several loss-of-function mutants for which we were unable to address the mechanism of action, such as synonymous mutations present in the *hok* CDS or in the 5' UTR. It is therefore decisive to construct individual mutants, to prove their viability and investigate individually their mechanism of action.

Third, the mutation $\Delta pSok$ lies in the *dcb* sequence (Supplementary Figure S4) and may render the *mok* SD/*dcb* stem less prone to be formed (one less GC pair). So, during the design of the experiment, it is important to keep in mind that mutating the promoter of the antitoxin can also affect the WT toxin mRNA sequence encoded on the opposite DNA strand.

Lastly, we investigated here a plasmidic T1TA not expressed from the chromosome, and validated the lack of cross-talk with chromosomal *hok*. In other studies, note that if the T1TA of interest is already present on the host chromosome, it should be deleted from the receiver strain before starting the investigation, and if a homologue is present in the host a possible cross-talk should be investigated.

CONCLUSIONS

A plethora of T1TA systems have been bioinformatically predicted in 2010 by Fozo *et al.*, but most of them have never been validated (32). Moreover, a precise characterization of the mechanism of action of the few systems studied in more detail is lacking. Here, we provide a genetic tool to study these mechanisms using high-throughput selection of single-nucleotide suppressor mutants of type I toxins in *E. coli*. T1TA toxicity has often been assessed under overexpression conditions. Our method is based on analyzing the chromosomal expression level of the toxin, thus securing against a potential toxic overexpression from a plasmid. This method, adapted from the FASTBAC-Seq of *H. pylori*, is based on uncovering loss-of-function mutants of the toxin by deep sequencing.

We validated our approach by revisiting the regulation of the well-characterized *hok/Sok* T1TA from *E. coli*. We obtained a good distribution of the substitutions over the locus and detected key regulatory elements embedded in the *hok* toxin mRNA at a nucleotide resolution. Then, we analyzed the mRNA and protein expression of several mutated transformants obtained during our preliminary analysis to validate our hypotheses concerning their mode of action. We found many *cis*-regulatory elements of the *hok/Sok* system that were already published, such as the promoter re-

gion, SD sequences and CDS boundaries, but also structural determinants found in the 5' and 3' UTRs. Indeed, comparably to what was published for *aapA3* (18), we detected here important nucleotides involved either in stabilizing structures that are not compatible with translation or in destabilizing translatable structures. This conformation equilibrium is characteristic of these T1TA systems for which the protein expression is regulated by a series of transient and final structures sequestering either the toxin SD sequence for *aapA3* or the *mok* leader peptide SD for *hok*. Finally, in addition to these already described regulatory determinants, we uncovered other substitutions for which the mechanism of action was not obvious or is still to be determined, such as synonymous amino acid substitutions in the *mok* and *hok* CDSs, but also substitutions in the 5' and 3' UTRs (Supplementary Figure S4, in red).

Compared to other methods that have been developed to study 5' UTRs, such as saturated mutagenesis followed by the monitoring of a reporter gene expression (33), our method is particularly adapted for the study of T1TAs. Although we are missing all mutations that have a positive effect on expression, we are not biased by the introduction of a reporter gene. Another major output provided by the use of FASTBAC-Seq is the capacity to reveal the conformational switch between the open and closed conformations of type I mRNAs. Therefore, we believe that our method could be suitable, with minor changes, for the study of other RNA structure-based systems, such as bacterial riboswitches and RNA thermometers. In these cases, a toxic CDS would be added downstream a library of mutated regulatory 5' UTRs, allowing life/death selection.

While identifying intragenic suppressors, our method does not enable the identification of *trans*-acting determinants regulating the systems although T1TAs are known to be regulated by RNA editing protein (*tadA*) and RNases (RNase III, PNPase, RNase II) (10–11,34). Therefore, it could be of interest to combine our method with the recently described toxin activation–inhibition conjugation method to identify extragenic activators and inhibitors of TA systems (35).

Taken together, we add a valuable tool in the field of T1TA research. Indeed, although they are produced as highly stable and not translatable molecules, toxin mRNAs are in a fragile balance between structures governing their activities; one single-nucleotide change can freeze a structure in the active translatable (open) or inactive (closed) state. With this study, we hope to provide a framework for a better analysis of the TA system determinants involved in toxin function and regulation. It will be helpful to study type I from many bacteria, and also the study of other TA types, in this case focusing on protein activity domains.

DATA AVAILABILITY

DNA sequencing data and results of differential statistical analyses have been deposited to NCBI GEO under the accession number GSE207195. All datasets generated in this study are available within the supplementary data.

SUPPLEMENTARY DATA

Supplementary Data are available at NAR Online.

ACKNOWLEDGEMENTS

We thank Donald Court laboratory for providing strains and plasmids for the *tetA-sacB* selection/counter-selection experiments. We acknowledge in particular Corentin Pelletan for technical help and Erwan Guichoux from the Plateforme Génome Transcriptome de Bordeaux. We acknowledge Thibaud Renault and Andrés Escalera Maurer for critical reading of the manuscript. We acknowledge all present and past members of the ARNA laboratory for helpful discussions.

FUNDING

INSERM (to ALR, NJT, SC and FD), Federation of European Biochemical Societies (to ALR), CNRS (to IO, ALR and FD), University of Bordeaux (to ALR, SB, FB and FD). Funding for open access charge: INSERM.

Conflict of interest statement. None declared.

REFERENCES

- Harms, A., Brodersen, D.E., Mitarai, N. and Gerdes, K. (2018) Toxins, targets, and triggers: an overview of toxin–antitoxin biology. *Mol. Cell*, **70**, 768–784.
- Masachis, S. and Darfeuille, F. (2018) Type I toxin–antitoxin systems: regulating toxin expression via Shine–Dalgarno sequence sequestration and small RNA binding. *Microbiol. Spectr.*, **6**, <https://doi.org/10.1128/microbiolspec.RWR-0030-2018>.
- Tourasse, N.J. and Darfeuille, F. (2021) T1TAdb: the database of type I toxin–antitoxin systems. *RNA*, **27**, 1471–1481.
- Gerdes, K., Rasmussen, P.B. and Molin, S. (1986) Unique type of plasmid maintenance function: postsegregational killing of plasmid-free cells. *Proc. Natl Acad. Sci. U.S.A.*, **83**, 3116–3120.
- Gerdes, K., Larsen, J.E. and Molin, S. (1985) Stable inheritance of plasmid R1 requires two different loci. *J. Bacteriol.*, **161**, 292–298.
- Thisted, T. and Gerdes, K. (1992) Mechanism of post-segregational killing by the *hok/sok* system of plasmid R1. *Sok* antisense RNA regulates *hok* gene expression indirectly through the overlapping *mok* gene. *J. Mol. Biol.*, **223**, 41–54.
- Gerdes, K., Bech, F.W., Jørgensen, S.T., Løbner-Olesen, A., Rasmussen, P.B., Atlung, T., Boe, L., Karlstrom, O., Molin, S. and von Meyenburg, K. (1986) Mechanism of postsegregational killing by the *hok* gene product of the *parB* system of plasmid R1 and its homology with the *relF* gene product of the *E. coli* *relB* operon. *EMBO J.*, **5**, 2023–2029.
- Steif, A. and Meyer, I.M. (2012) The *hok* mRNA family. *RNA Biol.*, **9**, 1399–1404.
- Thisted, T., Sørensen, N.S. and Gerdes, K. (1995) Mechanism of post-segregational killing: secondary structure analysis of the entire *hok* mRNA from plasmid R1 suggests a fold-back structure that prevents translation and antisense RNA binding. *J. Mol. Biol.*, **247**, 859–873.
- Franch, T., Gulyaev, A.P. and Gerdes, K. (1997) Programmed cell death by *hok/sok* of plasmid R1: processing at the *hok* mRNA 3'-end triggers structural rearrangements that allow translation and antisense RNA binding. *J. Mol. Biol.*, **273**, 38–51.
- Gerdes, K., Nielsen, A., Thorsted, P. and Wagner, E.G. (1992) Mechanism of killer gene activation. Antisense RNA-dependent RNase III cleavage ensures rapid turn-over of the stable *hok*, *srnB* and *pndA* effector messenger RNAs. *J. Mol. Biol.*, **226**, 637–649.
- Gulyaev, A.P., Franch, T. and Gerdes, K. (1997) Programmed cell death by *hok/sok* of plasmid R1: coupled nucleotide covariations reveal a phylogenetically conserved folding pathway in the *hok* family of mRNAs. *J. Mol. Biol.*, **273**, 26–37.
- Fozo, E.M. (2012) New type I toxin–antitoxin families from “wild” and laboratory strains of *E. coli*: Ibs-Sib, ShoB-OhsC and Zor-Orz. *RNA Biol.*, **9**, 1504–1512.
- Sharma, C.M., Hoffmann, S., Darfeuille, F., Reigier, J., Findeiß, S., Sittka, A., Chabas, S., Reiche, K., Hackermüller, J., Reinhardt, R. et al. (2010) The primary transcriptome of the major human pathogen *Helicobacter pylori*. *Nature*, **464**, 250–255.
- Maikova, A., Peltier, J., Boudry, P., Hajnsdorf, E., Kint, N., Monot, M., Poquet, I., Martin-Verstraete, I., Dupuy, B. and Soutourina, O. (2018) Discovery of new type I toxin–antitoxin systems adjacent to CRISPR arrays in *Clostridium difficile*. *Nucleic Acids Res.*, **46**, 4733–4751.
- Pichon, C. and Felden, B. (2005) Small RNA genes expressed from *Staphylococcus aureus* genomic and pathogenicity islands with specific expression among pathogenic strains. *Proc. Natl Acad. Sci. U.S.A.*, **102**, 14249–14254.
- Fraikin, N., Goormaghtigh, F. and Van Melderen, L. (2020) Type II toxin–antitoxin systems: evolution and revolutions. *J. Bacteriol.*, **202**, e00763-19.
- Masachis, S., Tourasse, N.J., Lays, C., Faucher, M., Chabas, S., Iost, I. and Darfeuille, F. (2019) A genetic selection reveals functional metastable structures embedded in a toxin-encoding mRNA. *eLife*, **8**, e47549.
- Masachis, S., Tourasse, N.J., Chabas, S., Bouchez, O. and Darfeuille, F. (2018) FASTBAC-Seq: functional analysis of toxin–antitoxin systems in bacteria by deep sequencing. *Methods Enzymol.*, **612**, 67–100.
- Li, X., Thomason, L.C., Sawitzke, J.A., Costantino, N. and Court, D.L. (2013) Positive and negative selection using the *tetA-sacB* cassette: recombineering and P1 transduction in *Escherichia coli*. *Nucleic Acids Res.*, **41**, e204.
- Thomason, L.C., Sawitzke, J.A., Li, X., Costantino, N. and Court, D.L. (2014) Recombineering: genetic engineering in bacteria using homologous recombination. *Curr. Protoc. Mol. Biol.*, **106**, 1.16.1–1.16.39.
- Schmieder, R. and Edwards, R. (2011) Quality control and preprocessing of metagenomic datasets. *Bioinformatics*, **27**, 863–864.
- Masella, A.P., Bartram, A.K., Truszkowski, J.M., Brown, D.G. and Neufeld, J.D. (2012) PANDAseq: paired-end assembler for Illumina sequences. *BMC Bioinformatics*, **13**, 31.
- Li, H. (2013) Aligning sequence reads, clone sequences and assemblycontigs with BWA-MEM. arXiv doi: <https://arxiv.org/abs/1303.3997>, 16 March 2013, preprint: not peer reviewed.
- Li, H., Handsaker, B., Wysoker, A., Fennell, T., Ruan, J., Homer, N., Marth, G., Abecasis, G. and Durbin, R. and 1000 Genome Project Data Processing Subgroup (2009) The Sequence Alignment/Map format and SAMtools. *Bioinformatics*, **25**, 2078–2079.
- Haas, B.J., Papanicolaou, A., Yassour, M., Grabherr, M., Blood, P.D., Bowden, J., Couger, M.B., Eccles, D., Li, B., Lieber, M. et al. (2013) *De novo* transcript sequence reconstruction from RNA-seq using the Trinity platform for reference generation and analysis. *Nat. Protoc.*, **8**, 1494–1512.
- Love, M.I., Huber, W. and Anders, S. (2014) Moderated estimation of fold change and dispersion for RNA-seq data with DESeq2. *Genome Biol.*, **15**, 550.
- Mutalik, V.K., Guimaraes, J.C., Cambray, G., Lam, C., Christoffersen, M.J., Mai, Q.-A., Tran, A.B., Paull, M., Keasling, J.D., Arkin, A.P. et al. (2013) Precise and reliable gene expression via standard transcription and translation initiation elements. *Nat. Methods*, **10**, 354–360.
- Hecht, A., Glasgow, J., Jaschke, P.R., Bawazer, L.A., Munson, M.S., Cochran, J.R., Endy, D. and Salit, M. (2017) Measurements of translation initiation from all 64 codons in *E. coli*. *Nucleic Acids Res.*, **45**, 3615–3626.
- Gulyaev, A.P., Franch, T. and Gerdes, K. (2000) Coupled nucleotide covariations reveal dynamic RNA interaction patterns. *RNA*, **6**, 1483–1491.
- Tourasse, N.J. and Darfeuille, F. (2020) Structural alignment and covariation analysis of RNA sequences. *Bio Protoc.*, **10**, e3511.
- Fozo, E.M., Makarova, K.S., Shabalina, S.A., Yutin, N., Koonin, E.V. and Storz, G. (2010) Abundance of type I toxin–antitoxin systems in bacteria: searches for new candidates and discovery of novel families. *Nucleic Acids Res.*, **38**, 3743–3759.
- Holmqvist, E., Reimegård, J. and Wagner, E.G.H. (2013) Massive functional mapping of a 5'-UTR by saturation mutagenesis, phenotypic sorting and deep sequencing. *Nucleic Acids Res.*, **41**, e122.
- Bar-Yaacov, D., Mordret, E., Towers, R., Biniashvili, T., Soyris, C., Schwartz, S., Dahan, O. and Pilpel, Y. (2017) RNA editing in bacteria recodes multiple proteins and regulates an evolutionarily conserved toxin–antitoxin system. *Genome Res.*, **27**, 1696–1703.
- Bobonis, J., Mitosch, K., Mateus, A., Karcher, N., Kritikos, G., Selkris, J., Zietek, M., Monzon, V., Pfalz, B., Garcia-Santamarina, S. et al. (2022) Bacterial retrons encode phage-defending tripartite toxin–antitoxin systems. *Nature*, **609**, 144–150.